

Conundrum of weak-noise limit for diffusion in a tilted periodic potential

J. Spiechowicz* and J. Łuczka

Institute of Physics, University of Silesia, 41-500 Chorzów, Poland

(Received 23 June 2021; accepted 20 August 2021; published 7 September 2021)

The weak-noise limit of dissipative dynamical systems is often the most fascinating one. In such a case fluctuations can interact with a rich complexity, frequently hidden in deterministic systems, to give rise to phenomena that are absent for both noiseless and strong fluctuations regimes. Unfortunately, this limit is also notoriously hard to approach analytically or numerically. We reinvestigate in this context the paradigmatic model of nonequilibrium statistical physics consisting of inertial Brownian particles diffusing in a tilted periodic potential by exploiting state-of-the-art computer simulations of an extremely long timescale. In contrast to previous results on this longstanding problem, we draw an inference that in the parameter regime for which the particle velocity is bistable the lifetime of ballistic diffusion diverges to infinity when the thermal noise intensity tends to zero, i.e., an everlasting ballistic diffusion emerges. As a consequence, the diffusion coefficient does not reach its stationary constant value.

DOI: [10.1103/PhysRevE.104.034104](https://doi.org/10.1103/PhysRevE.104.034104)**I. INTRODUCTION**

Deterministic nonlinear dynamical systems are of paramount importance due to their vast applications in a broad spectrum of scientific disciplines [1]. Their nonlinear nature allows for a rich complexity which is not present in linear systems. One of the reasons behind it is the validity of the superposition principle for linear systems, which states that the response caused by two or more perturbations is the sum of the reactions that would have been induced by each stimulus individually. Nonlinear setups are known to exhibit unusual behavior such as chaos, in which the deterministic nature of a system does not make it predictable [2]; multistability, when two or more stable states are present in the setup dynamics [3]; limit cycles, the existence of asymptotic periodic orbits to which a perturbed system is attracted [1]; and solitons, self-reinforcing wave packets [4], to name only a few.

On the other hand, in the past four decades it has been understood that noise can produce qualitative changes in the properties of a deterministic system [5]. Random fluctuations acting upon a nonlinear setup out of equilibrium may have particularly far-reaching consequences. This is due to the fact that equilibrium is ruled by various thermodynamic laws and symmetries, e.g., detailed balance, which generally lose their validity out of equilibrium. There are two main ways in which noise can interact with nonlinearity to render counterintuitive behavior. First, fluctuations can help a multistable system cross a potential barrier separating different stable states. If, for a finite dose of noise, the random crossing times statistically match a deterministic timescale of the system, a more regular behavior may emerge, e.g., in the form of (quasi)periodicity. This is the basic mechanism standing

behind phenomena such as stochastic resonance [6,7] and coherence resonance [8,9]. Second, fluctuations can destabilize stationary states existing in the nonlinear dynamics and induce new states which could correspond to qualitatively and quantitatively different evolution. The latter observation is the *modus operandi* of phenomena like noise-induced transport [10,11], negative mobility [12–15], or recently discovered fluctuation-induced dynamical localization [16,17] causing anomalous diffusion [18] in systems which at the first glance cannot react in this way.

In this context, particularly interesting is a limiting situation of weak noise interacting with a deterministic nonlinear system. When the intensity of fluctuations is too high they usually smear the dynamics too much so that the impact of deterministic evolution is barely visible if not completely irrelevant. In this way a rich complexity often hidden in a noiseless nonlinear system is destroyed. Unfortunately, the weak-noise limit is also notoriously hard to approach. Dynamical systems under the influence of fluctuations are often successfully modeled by the Fokker-Planck equation [19] whose time-independent solutions corresponding to the steady states are the most relevant. Mathematically, the weak-noise limit of the time-independent solutions of the Fokker-Planck equation is the most problematic one. The reason is that then actually two limits are involved: Time tends to infinity, in which the steady state is approached, and the weak-noise limit must be carried out after the limit $t \rightarrow \infty$.

In this paper we reinvestigate the paradigmatic model of nonequilibrium statistical physics, namely, underdamped Brownian motion in a biased periodic potential to analyze diffusion in the weak-noise limit. This setup is isomorphic with many important physical systems [19] such as the Josephson junction [20], dipoles rotating in external fields [21], superionic conductors [22], charge density waves [23], and cold atoms dwelling in optical lattices [24], to mention only a few. In view of the above discussion, it is not surprising that the

*jakub.spiechowicz@us.edu.pl

asymptotic analytical methods have not yet been elaborated for this system and one needs to rely solely on numerical results. Consequently, there are many mutually contradictory results in the literature concerning the conundrum of the weak-noise limit for diffusion in a tilted periodic potential. Here we exploit the state-of-the-art computer simulations of an extremely long timescale to draw an inference about this longstanding problem.

The paper is organized as follows. In Sec. II we recall the formulation of the model and introduce the dimensionless quantities. In Sec. III we describe the basic features of the deterministic dynamics. In Sec. IV we introduce the diffusion quantifiers and discuss the state of the art of the weak-noise limit. In Sec. V we first comment on the everlasting anomalous diffusion occurring in this system. Next we debate the weak-ergodicity breaking and the relation between the diffusion coefficient and the residence probabilities in two states of the velocity dynamics. In Sec. VI we discuss the finite-time measurements of the diffusion coefficient that is important from an experimental point of view. Section VII provides a summary and conclusions.

II. MODEL

In this paper we revisit the problem of diffusion in a tilted periodic (also named washboard) potential. We consider a classical Brownian particle of mass M , moving in a spatially periodic and symmetric potential $U(x) = U(x + L)$ of period L and subjected to a constant biasing force F . The dynamics of this system can be described by the Langevin equation

$$M\ddot{x} + \Gamma\dot{x} = -U'(x) + F + \sqrt{2\Gamma k_B T}\xi(t), \quad (1)$$

where the overdot and the prime denote differentiation with respect to time t and the particle coordinate x , respectively. The parameter Γ is the friction coefficient and k_B is the Boltzmann constant. The spatially periodic potential $U(x)$ is assumed to be in one of the simplest forms, namely,

$$U(x) = -\Delta U \sin\left(\frac{2\pi}{L}x\right), \quad (2)$$

where ΔU is half of the barrier height and L is the spatial period. Thermal fluctuations due to the coupling of the particle with the thermal bath of temperature T are modeled by δ -correlated Gaussian white noise $\xi(t)$ of zero mean and unit intensity, i.e.,

$$\langle \xi(t) \rangle = 0, \quad \langle \xi(t)\xi(s) \rangle = \delta(t - s). \quad (3)$$

The noise intensity factor $2\Gamma k_B T$ in Eq. (1) follows from the fluctuation-dissipation theorem [25], which ensures that the equilibrium counterpart of the system given by Eq. (1) obeys the canonical Gibbs statistics.

In physics only the relations between scales of time, length, and energy appearing in physical laws but not their absolute values play a crucial role in determining the progress of observed phenomena. Therefore, as the first step we transform Eq. (1) into its dimensionless form. This aim can be achieved in several ways depending on the choice of the timescale [26]. Here we define the dimensionless coordinate \hat{x} and

dimensionless time \hat{t} in the following manner:

$$\hat{x} = \frac{2\pi}{L}x, \quad \hat{t} = \frac{t}{t_1}, \quad t_1 = \frac{L}{2\pi} \sqrt{\frac{M}{\Delta U}}. \quad (4)$$

The characteristic time t_1 is the inverse of frequency of small oscillations in the well of the potential $U(x)$.

Under the above scaling, Eq. (1) is transformed to the form

$$\ddot{\hat{x}} + \gamma\dot{\hat{x}} = \cos\hat{x} + f + \sqrt{2\gamma\theta}\hat{\xi}(\hat{t}), \quad (5)$$

where now the overdot denotes differentiation with respect to dimensionless time \hat{t} . We note that the dimensionless mass is $m = 1$ and the remaining rescaled parameters are

$$\gamma = \frac{t_1}{t_2} = \frac{1}{2\pi} \frac{L}{\sqrt{M\Delta U}}\Gamma, \quad f = \frac{1}{2\pi} \frac{L}{\Delta U}F. \quad (6)$$

The second characteristic time is $t_2 = M/\Gamma$, which for a free Brownian particle defines the velocity relaxation time. The rescaled temperature θ is given by the ratio of thermal energy $k_B T$ to half of the activation energy the particle needs to overcome the original potential barrier ΔU , i.e.,

$$\theta = \frac{k_B T}{\Delta U}. \quad (7)$$

The dimensionless thermal noise $\hat{\xi}(\hat{t})$ assumes the same statistical properties as $\xi(t)$, namely, it is a Gaussian stochastic process with vanishing mean $\langle \hat{\xi}(\hat{t}) \rangle = 0$ and the correlation function $\langle \hat{\xi}(\hat{t})\hat{\xi}(\hat{s}) \rangle = \delta(\hat{t} - \hat{s})$. From now on we will use only the dimensionless variables and will omit the hat in all quantities appearing in the Langevin equation (5).

III. DETERMINISTIC DYNAMICS

We recall the basic transport properties of the deterministic counterpart of the system, i.e., when $\theta = 0$. For sufficiently large friction coefficient, we can neglect the inertial effects, namely, omit the \ddot{x} term in Eq. (5). Then in the deterministic limit the particle performs a creeping motion. If the tilted potential $\mathcal{U}(x) = -\sin x - fx$ exhibits minima, the particle is pinned in the local minimum at large time and its average velocity is $\mathbb{E}[v] = 0$, where

$$\mathbb{E}[v] = \lim_{t \rightarrow \infty} \frac{1}{t} \int_0^t ds \dot{x}(s) \quad (8)$$

stands for a time-averaged velocity for a single trajectory of the system. This solution is termed the locked state. If the bias f is large enough and minima cease to exist, the particle slides down the tilted potential $\mathcal{U}(x)$ and its average velocity is nonzero $\mathbb{E}[v] > 0$. Such a solution is termed the running state. For a smaller friction coefficient inertial effects become significant. If the potential $\mathcal{U}(x)$ minima exist in this regime, the locked solution may emerge. Moreover, because of inertia, the Brownian particle may overcome the potential barriers if the damping is small enough and the running solutions can occur. Such a regime is called bistable and the occurrence of the locked or running state depends on the particle's initial state. This effect is well known since the work of Vollmer and Risken [27]. To observe average velocity bistability, for a given friction coefficient the constant force must be in the range $f_1(\gamma) < f < f_3 = 1$, where f_1 is the minimal value for

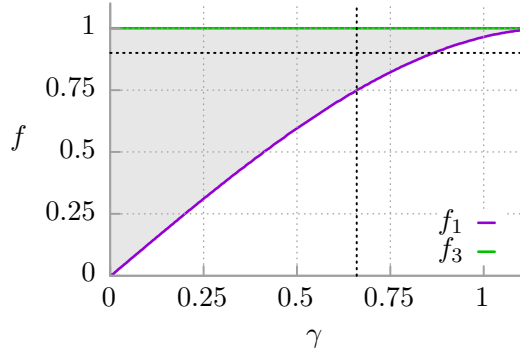


FIG. 1. Phase diagram for the occurrence of the velocity bistability phenomenon in the deterministic system presented in the dimensionless parameter plane (γ, f) . Due to this effect, in the gray area, the ballistic diffusion emerges in the deterministic limit of vanishing temperature. The dashed horizontal and vertical lines correspond to $f = 0.9$ and $\gamma = 0.66$, respectively. This regime is analyzed in the paper.

which the running state starts to appear for the deterministic system [19]. In Fig. 1 we reproduce the phase diagram for the occurrence of the average velocity bistability phenomenon in the dimensionless parameter plane (γ, f) . This effect is observed only if the bias f lies in the gray area.

IV. OVERVIEW OF DIFFUSION IN A WASHBOARD POTENTIAL

A. Diffusion quantifiers

The most fundamental quantity characterizing the diffusion process is the mean square deviation (variance) of the particle coordinate $x(t)$, namely [19],

$$\langle \Delta x^2(t) \rangle = \langle [x(t) - \langle x(t) \rangle]^2 \rangle = \langle x^2(t) \rangle - \langle x(t) \rangle^2, \quad (9)$$

where $\langle \cdot \rangle$ indicates averaging over all thermal noise realizations as well as over initial conditions for the position $x(0)$ and velocity $v(0) = \dot{x}(0)$ of the Brownian particle. In the long-time limit the variance typically becomes an increasing function of the elapsing time [18]

$$\langle \Delta x^2(t) \rangle \sim t^\alpha. \quad (10)$$

The exponent α specifies the diffusion process. Normal diffusion is observed for $\alpha = 1$. The case $0 < \alpha < 1$ is termed subdiffusion, while $\alpha > 1$ describes superdiffusion [18].

One can also define the time-dependent diffusion coefficient $D(t)$ as [28]

$$D(t) = \frac{\langle \Delta x^2(t) \rangle}{2t}. \quad (11)$$

Note that the time-decreasing $D(t)$ corresponds to subdiffusion, whereas superdiffusion occurs when $D(t)$ increases. When the exponent α approaches unity $D(t) = \text{const}$ and we deal with normal diffusion [28], i.e.,

$$D = \lim_{t \rightarrow \infty} D(t) < \infty. \quad (12)$$

As a result, the diffusive behavior of the system is fully characterized only by specifying both the power exponent α and the diffusion coefficient $D(t)$.

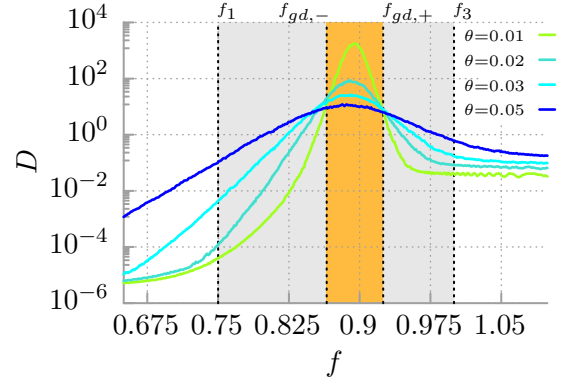


FIG. 2. Diffusion coefficient D versus bias f for different values of temperature θ of the system. The gray shaded region shows the interval $[f_1, f_3]$ where, in the deterministic system, the bistability of the velocity dynamics occurs. The orange regions shows the critical bias f range $[f_{gd,-}, f_{gd,+}]$ for which, according to the two-state theory presented in [50], the diffusion coefficient tends to infinity $D \rightarrow \infty$ when temperature vanishes $\theta \rightarrow 0$. The dimensionless friction coefficient is $\gamma = 0.66$.

B. Riddle of weak-noise limit

The study of various aspects of Brownian motion in a washboard potential has a long history (see, e.g., [19]). This system constitutes a beautiful paradigm of a simple nonlinear system exhibiting interesting classical and quantum phenomena and still remains a vibrant topic of current research [29–40]. The reason behind it is its underlying complexity, which at the first glance is unnoticeable. Remember that the Fokker-Planck equation for the particle probability distribution $P(x, v, t)$ corresponding to Eq. (5) is a second-order partial differential equation of a parabolic type whose parameter space is three dimensional $\{\gamma, f, \theta\}$ and exact solutions are generally unattainable. Nevertheless, some interesting asymptotic and/or limiting cases have been investigated and analytically solved (see, e.g., [19,41–46]).

Despite many years of active research on this system, one problem still remains unsolved: the weak-noise limit for diffusion in a tilted periodic potential. Amplification of diffusion D by orders of magnitude over the bare diffusion coefficient $D_0 = \theta/\gamma$ of a free particle was first observed over 20 years ago in [47]. The authors attributed it to bistability of the velocity dynamics and reported the bell-shaped dependence of the diffusion coefficient on the constant force. In Ref. [48] it was suggested that the maximal diffusion coefficient D_{max} grows with inverse temperature like a power law $D_{\text{max}} \sim T^{-3.5}$ and that the force range of diffusion enhancement shrinks to zero when approaching zero temperature $\theta \rightarrow 0$. It was disputed in [49], where it was argued that the increase of D follows rather an exponential dependence on the inverse temperature $D_{\text{max}} \sim T^{2/3} \exp(\epsilon/k_B T)$, where ϵ is an effective barrier for the bistable velocity dynamics. Moreover, the authors reported that when temperature decreases to zero the diffusion coefficient D tends to zero as well (strong-damping regime) or it increases (weak-damping regime). In Ref. [50] a two-state theory was used to determine, for all values of the friction coefficient γ , the range of forces $[f_{gd,-}, f_{gd,+}]$ (cf. Fig. 2) in which the diffusion coefficient increases to infinity as

temperature decreases to zero, $D_{\max} \sim T^{0.22} \exp(\epsilon/k_B T)$. The authors also indicated that, outside this interval, D possesses a pronounced maximum as a function of temperature and it goes exponentially to zero for $\theta \rightarrow 0$. The width of the orange region of giant enhancement of diffusion was found to be a nonmonotonic function of the friction coefficient γ possessing a distinct maximum. The last claim was discussed later in [51,52], where the dependence of D on various parameters of the model was discussed and it was suggested that the width of this interval decreases linearly with γ . Finally, very recently we [53] followed a different approach and focused on moderate- to high-temperature regimes to construct a phase diagram for the occurrence of the nonmonotonic temperature dependence of the diffusion coefficient. The latter result extends the predictions contained in [50]; however, it barely touches the weak-thermal-noise limit. Finally, in Ref. [54] we show that the real-time velocity dynamics in this system is not bistable but rather multistable.

The above brief discussion illustrates that the conundrum of a zero-temperature limit for diffusion in a tilted periodic potential has still not been satisfactorily resolved and there are many mutually contradictory results in the literature. The reason behind it probably lies in the fact that transitions between the velocity states are driven by thermal noise whose intensity is $\gamma\theta$. Therefore, regimes of low damping γ and/or temperature θ require exponentially larger simulation times to sample the state space of the system reliably. Preferably, asymptotic analytical methods should be employed; however, these have not yet been developed. In this paper we want to debate the longstanding issue of the weak-thermal-noise limit by exploiting the state-of-the-art computer simulations of an extremely long timescale (discussed below).

V. RESULTS

Since we cannot solve analytically the Fokker-Planck equation corresponding to Eq. (5) we had to resort to comprehensive numerical simulations. All numerical calculations have been done by the use of a compute unified device architecture environment implemented on a modern desktop graphics processing unit (GPU). This procedure allowed for a speedup of a factor of the order of 10^3 times as compared to the present-day central processing unit method [55]. The quantities characterizing the diffusive behavior of the system were averaged over the ensemble of 10^5 trajectories, each starting with different initial condition $x(0)$ and $v(0)$ distributed uniformly over the intervals $[0, 2\pi]$ and $[-2, 2]$, respectively.

The Langevin equation (5) was integrated using a second-order predictor-corrector scheme [56] with the time step $h = 10^{-2}$. Since we are interested not only in a short time behavior of the system, but also its asymptotic state, numerical stability is an extremely important problem to obtain reliable results. Hopefully, the predictor-corrector algorithm is similar to implicit methods but does not require the solution of an algebraic equation at each step. It offers good numerical stability, which it inherits from the implicit counterpart of its corrector.

Each trajectory of the system was associated with its own random number generator, which guaranteed independence

of the noise term between different realizations. Initial random number generator seeds were chosen randomly using a standard integer random generator available on the host. On the GPU we implemented an XOR-shift random number generator that allowed for a particularly efficient execution requiring a very small code and state. Its parameters were chosen carefully in order to achieve a period $2^{64} - 1$, which is more than enough for this type of task.

A. Everlasting anomalous diffusion

The deterministic counterpart of the setup exhibits the bistable velocity dynamics if for a given friction γ the bias is in the range $f_1(\gamma) < f < f_3 = 1$. When $f < f_1(\gamma)$ only the locked solution emerges, while for $f > f_3$ the running state occurs exclusively. Therefore, for these regions there exists only one class of trajectories $\langle x(t) \rangle \sim \mathbb{E}[v]t$, with $\mathbb{E}[v] = 0$ or $\mathbb{E}[v] > 0$, respectively. Consequently, there is no spread of trajectories and the diffusion coefficient must vanish outside the gray region in Fig. 1, i.e., $D = 0$ when $\theta = 0$ and likewise $D \rightarrow 0$ if $\theta \rightarrow 0$. In the bistable region (inside the gray area) the diffusion is ballistic in the deterministic regime. The contribution comes from the spread between the locked and running trajectories and formally $D = \infty$ in Eq. (12). If the temperature is nonzero, the diffusion coefficient D is nonzero and finite in all three intervals of the bias $f < f_1$, $f \in [f_1, f_3]$, and $f > f_3$. In the rest of the paper we limit our study to the interval $[f_1, f_3]$, where the bistability of the velocity dynamics occurs and for which there is no consensus on the weak-noise limit.

In Fig. 3 we present the most basic characteristics describing the diffusive behavior of the system, namely, the time-dependent diffusion coefficient $D(t)$ defined in Eq. (11), which surprisingly has been missed in most of the recent studies concerning this issue. It is depicted there for the fixed representative friction $\gamma = 0.66$ (cf. Fig. 1) and different values of the dimensionless temperature θ of the system coded via the corresponding color. In Fig. 3(a) we show this characteristic for the subcritical bias $f = 0.85 \in [f_1, f_{gd,-}]$, in Fig. 3(b) the force taken from the critical region $f = 0.9 \in [f_{gd,-}, f_{gd,+}]$, and in Fig. 3(c) the supercritical bias $f = 0.94 \in [f_{gd,+}, f_3]$ (cf. Fig. 2). We note that the timescale of the presented evolution spans nine orders of magnitude of the characteristic unit of time. One can observe there two distinct regimes. The first one is visible in Fig. 3(b), i.e., for the bias $f = 0.9$ (see Fig. 1) lying in the critical interval $[f_{gd,-}, f_{gd,+}]$. In this regime $D(t)$ monotonically tends to its time-independent stationary value D . First there is an initial stage $(0, \tau_1)$ of ballistic diffusion when the diffusion coefficient increases linearly (note that the scale is logarithmic for both axes) and next, for $t > \tau_1$, normal diffusion is approached. On the other hand, the second regime is observed for the sub- and supercritical biases f [cf. Figs. 3(a) and 3(c)], where, except at high temperature θ , the diffusion coefficient $D(t)$ displays nonmonotonic relaxation towards its stationary value. In the initial interval $(0, \tau_1)$ the diffusion coefficient $D(t)$ grows with time in a ballistic manner; next there is an extended window (τ_1, τ_2) when it decreases, indicating subdiffusion; and for $t > \tau_2$ it finally reaches its steady state. For sufficiently high temperature the relaxation pattern

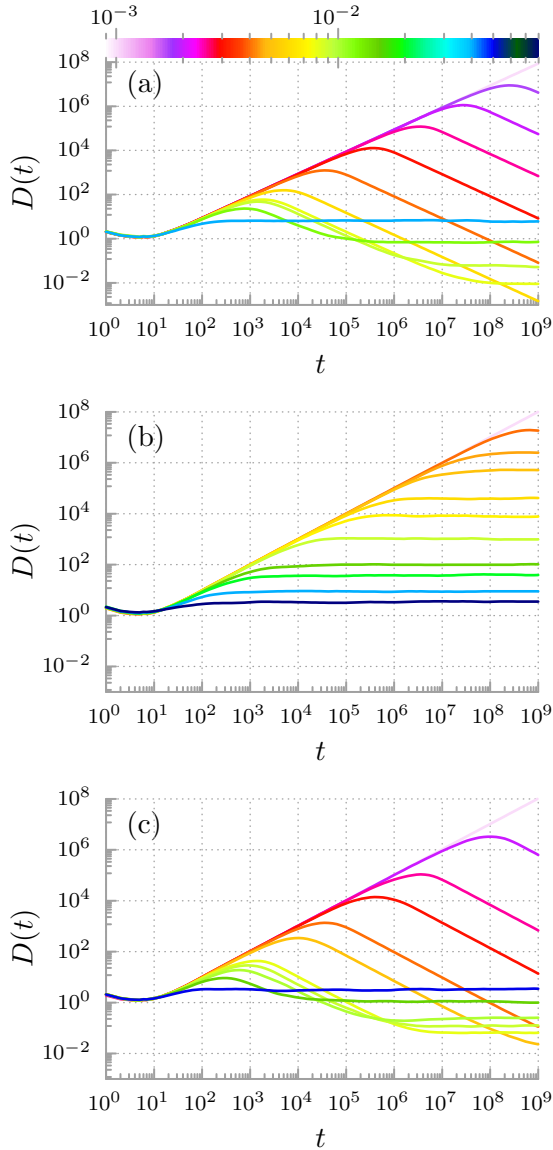


FIG. 3. Trajectory of the diffusion coefficient $D(t)$ depicted for different (color-coded) values of the dimensionless temperature θ of the system, with (a) subcritical force $f = 0.85 \in [f_1, f_{gd,-}]$, (b) critical bias $f = 0.9 \in [f_{gd,-}, f_{gd,+}]$, and (c) supercritical force $f = 0.94 \in [f_{gd,+}, f_3]$ (cf. Fig. 2). The friction coefficient is $\gamma = 0.66$.

of $D(t)$ is monotonic and the same as in the critical bias range $[f_{gd,-}, f_{gd,+}]$.

Moreover, there are other similarities which are presented in Fig. 4, where we depict the influence of temperature θ on the crossover times τ_1 and τ_2 of the ballistic motion and subdiffusion, respectively. If the temperature decreases $\theta \rightarrow 0$ the time interval of ballistic diffusion rapidly increases and tends to infinity $\tau_1 \rightarrow \infty$ regardless of the magnitude of the bias f . This picture is consistent with the deterministic limit $\theta = 0$, where in the entire interval $[f_1, f_3]$ the velocity bistability effect occurs, which serves as the backbone of the persistent ballistic diffusion $D(t) \rightarrow \infty$. However, as it is displayed in the figure, the crossover time τ_1 depends on the static force f . In the critical interval $[f_{gd,-}, f_{gd,+}]$ it is much larger than outside it, e.g., for temperature $\theta = 0.006$ the lifetime of

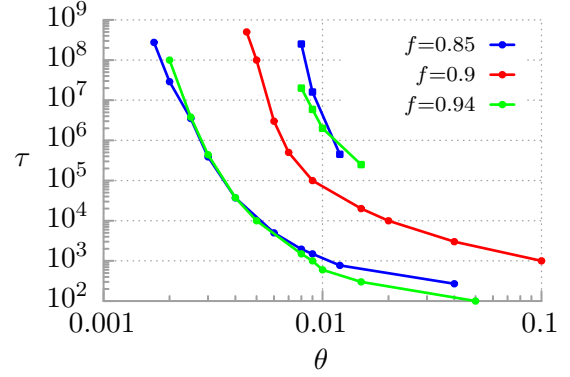


FIG. 4. Crossover times τ_1 (solid lines) and τ_2 (dashed lines) of the ballistic motion and subdiffusion, respectively, versus the temperature θ of the system for the subcritical $f = 0.85$, critical $f = 0.9$, and supercritical $f = 0.94$ biases.

ballistic diffusion is $\tau_1 \approx 10^7$ for the critical bias $f = 0.9 \in [f_{gd,-}, f_{gd,+}]$ and $\tau_1 \approx 10^4$ for both the subcritical $f = 0.85 \in [f_1, f_{gd,-}]$ and the supercritical $f = 0.94 \in [f_{gd,+}, f_3]$ force. We note that the crossover time τ_1 is similar for the subcritical and supercritical bias values. The time span of our computer simulations allowed us to estimate even the crossover time τ_2 of subdiffusion occurring outside the critical interval $[f_{gd,-}, f_{gd,+}]$. For instance, for temperature $\theta = 0.01$ the lifetime of ballistic diffusion is $\tau_1 \approx 10^3$, whereas the crossover time of subdiffusion is $\tau_2 \approx 10^7$. Therefore, the duration of the observed transient anomalous diffusive behavior is extremely sensitive to temperature variation. Unfortunately, even though our state-of-the-art computational method allowed us to explore an exceptionally long timescale of the system evolution, we are still far from the truly low-temperature regimes. Our results reveal that already for moderate thermal noise intensity $\theta \approx 0.001$ the lifetime of the ballistic diffusion $\tau_1 > 10^9$. However, certainly they are sufficient to draw an inference about the conundrum of the weak-thermal-noise limit for diffusion in a tilted periodic potential.

One can note that the everlasting anomalous diffusion and the lifetime τ_1 of superdiffusion can be explained in terms of eigenvalues of the Fokker-Planck equation corresponding to the Langevin equation (1). In Fig. 11.43(a) in Ref. [19], the two lowest eigenvalues (say, λ_0 and λ_1) are depicted in dependence on the bias f . The eigenvalues correspond to characteristic times of the system and determine the rate of approaching the stationary state and various stationary expectation values. The crucial feature is that inside of the bistability region, λ_0 decreases to zero when temperature decreases to zero and λ_1 approaches a nonzero value. This means that the characteristic time $\tau_0 = 1/\lambda_0 \rightarrow \infty$ when $\theta \rightarrow 0$. This time can be identified with the lifetime τ_1 of superdiffusion, i.e., $\tau_1 \sim 1/\lambda_0$. It should be pointed out that in the case of overdamped dynamics, the behavior of eigenvalues as a function of the bias f is different (cf. Fig. 3 in Ref. [39]).

The results shown in Fig. 3 suggest that the time-dependent diffusion coefficient $D(t)$ could be described by the relation

$$D(t) \sim D + E(t), \quad (13)$$

where D is a steady-state constant diffusion coefficient defined by Eq. (12). The function $E(t)$ has the following properties: (i) $E(t) \rightarrow 0$ when $t \rightarrow \infty$ for any $\theta \neq 0$ and (ii) its maximum $E_{\max} = E(\tau_1) \rightarrow \infty$ and $\tau_1 \rightarrow \infty$ when $\theta \rightarrow 0$, where τ_1 is the lifetime of ballistic diffusion. Even if for $f \in [f_{gd,-}, f_{gd,+}]$ the diffusion coefficient $D = D(\theta) \rightarrow \infty$ when $\theta \rightarrow 0$ and for $f \in [f_1, f_{gd,-}]$ or $f \in [f_{gd,+}, f_3]$ the diffusion coefficient $D = D(\theta) \rightarrow 0$ when $\theta \rightarrow 0$, the function $D(t) \rightarrow \infty$ as $\theta \rightarrow 0$ and in practice it does not make sense to ask about the value of D in the limit $\theta \rightarrow 0$ because then D is not well defined.

B. Weak-ergodicity breaking

For any nonzero temperature $\theta > 0$ the system (5) is ergodic, although the ergodicity is nontrivial since it is driven by a degenerate noise [45]. At very low temperature the whole phase space is still accessible because of thermally activated escape events connecting coexisting deterministic disjoint attractors; however, the time after it is fully sampled is extremely long. If temperature tends to zero $\theta \propto T \rightarrow 0$ the crossover time of superdiffusion monotonically increases to infinity $\tau_1 \rightarrow \infty$ and ergodicity is broken. In experiments there is not much difference whether the system is nonergodic or ergodic but exhibiting an unusually slow relaxation towards its steady state. The latter situation occurring here is often captured as weak-ergodicity breaking [57]. It can be characterized by the Deborah number De [58],

$$De = \frac{\tau}{\mathcal{T}}, \tag{14}$$

which is the ratio of a relaxation time τ of a given observable and the time of observation \mathcal{T} . In the case of weak-ergodicity breaking it diverges $De \rightarrow \infty$. This can happen not only because \mathcal{T} is short but also because τ is enormously long. In our case the system behaves as weakly nonergodic for the mean square deviation of the particle coordinate when the superdiffusion lifetime $\tau = \tau_1 \sim 1/\lambda_0$ is sufficiently large. As we demonstrate in Fig. 4, this condition is quickly satisfied when temperature θ goes down to zero.

C. Residence probabilities

The properties of the diffusion coefficient D shown in Fig. 2 can be reformulated in terms of the stationary probabilities p_l and p_r of finding the particle in the locked ($\mathbb{E}[v] = 0$) and running ($\mathbb{E}[v] > 0$) states, respectively. Let us define the quantifier $Q = 1 - |p_l - p_r|$, which, roughly speaking, characterizes the difference between the number of locked and running trajectories. We note that when $Q \neq 0$ the locked and running solutions coexist. If $p_l = p_r$, i.e., when both trajectories are equiprobable, then Q attains its maximal value $Q = 1$.

For the bistable velocity dynamics and any fixed nonzero temperature θ there are three contributions to the spread of trajectories of the system around its mean path and consequently to the diffusion coefficient D . The first, which is the leading one, is associated with the spread coming from the relative distance between the locked and running solutions. The second and third contributions are related to thermal-noise-induced spread of trajectories following the locked and running trajectories, respectively. The diffusion coefficient D is maximal when the share of the first contribution is

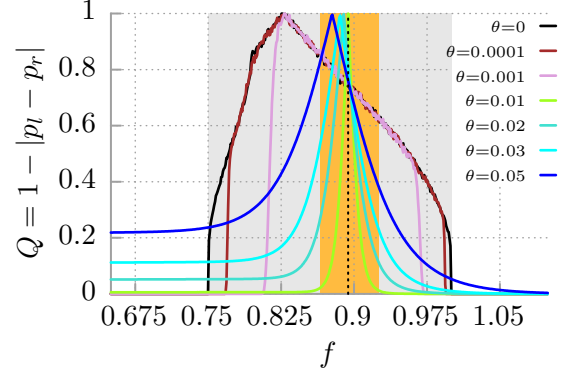


FIG. 5. Difference $Q = 1 - |p_l - p_r|$ between the stationary probability p_l and p_r of finding the particle in the locked ($\mathbb{E}[v] = 0$) and running ($\mathbb{E}[v] > 0$) states, respectively, versus the bias f for different values of the temperature θ of the system. The gray shaded region shows the interval $[f_1, f_3]$ where, in the deterministic system, the bistability of the velocity dynamics occurs. The orange region shows the critical bias f range $[f_{gd,-}, f_{gd,+}]$ for which, according to the two-state theory presented in [50], the diffusion coefficient tends to infinity $D \rightarrow \infty$ when temperature vanishes $\theta \rightarrow 0$. The dimensionless friction coefficient is $\gamma = 0.66$.

peaked. This is the case for the equiprobable locked and running trajectories, i.e., when $Q = 1$. We note that in the zero-temperature limit $\theta \rightarrow 0$ the second and third contributions die out and only the first survives. Consequently, the diffusion is ballistic. We exemplify the above observations in Fig. 5 for $\theta = 0.01$ by the vertical dashed line pointing at $f = 0.894$, where the corresponding curve $D(f)$ in Fig. 2 is maximal. The resonancelike shape of the quantifier Q provides an elegant yet insightful explanation for the giant diffusion effect which has been overlooked in the literature. Moreover, we pay attention to the fact that the bias f region where the velocity bistability occurs is significantly modified by temperature θ . When $\theta \rightarrow 0$ it tends to $[f_1, f_3]$ and not to $[f_{gd,-}, f_{gd,+}]$. We observe that for vanishing thermal noise intensity the number of locked and running trajectories in $[f_1, f_3]$ is of the same order and $|p_l - p_r|$ is relatively small. Consequently, $\langle x(t) \rangle \sim \langle v \rangle t$, the leading term in the mean square displacement, is $\langle \Delta x^2(t) \rangle \sim t^2$ and one observes the persistent ballistic diffusion with $D(t) \rightarrow \infty$. Its constancy is guaranteed via the strong-ergodicity breaking [54,57], i.e., there are two mutually inaccessible attractors for the average velocity of the particle in the phase space of the system.

VI. FINITE-TIME MEASUREMENTS

The timescale of the actual physical experiment is always limited and therefore in the considered case it is useful to analyze the finite-time diffusion coefficient $D(t = t_i)$. This characteristic is depicted in Fig. 6 for $t_i = 10^6$ as a function of the temperature θ of the system and the subcritical, critical, and supercritical forces f . For sufficiently high temperature θ the Einstein relation $D \propto \theta$ must be recovered, as then thermal noise dominates the right-hand side of Eq. (5) and the particle behaves as a free one. Due to the bistability of the velocity dynamics when temperature θ is lowered,

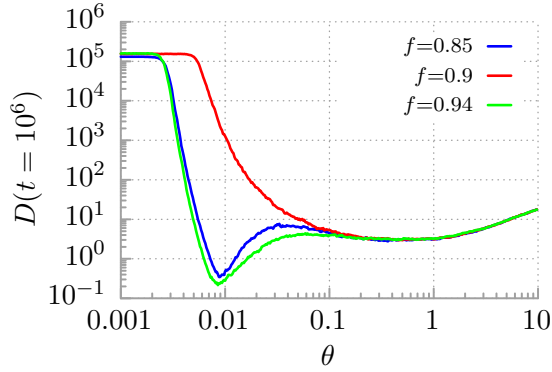


FIG. 6. Finite-time diffusion coefficient $D(t = t_i = 10^6)$ versus the temperature θ of the system for the subcritical, critical, and supercritical biases f .

we observe a distinctive nonmonotonic temperature dependence of the diffusion coefficient $D(t_i)$. We note that the number of diffusion extrema is determined by the magnitude of the bias f acting on the particle. For the critical tilt $f = 0.9 \in [f_{gd,-}, f_{gd,+}]$ there is only one minimum, whereas for the subcritical force $f = 0.85 \in [f_1, f_{gd,-}]$ and supercritical force $f = 0.94 \in [f_{gd,+}, f_3]$ both minima and maxima are attainable. However, when we keep lowering temperature eventually the diffusion coefficient $D(t_i)$ saturates on the plateau corresponding to the ballistic diffusion $D(t_i) = D_b(t_i) \sim t_i$. We conclude that in physics limits are often noncommutative. This is the case for diffusion in the tilted periodic potential when the velocity bistability occurs for $f \in [f_1(\gamma), f_3]$. Then (i) if temperature goes down to zero $\theta \rightarrow 0$ and time tends to infinity $t \rightarrow \infty$, the lifetimes of the superdiffusion $\tau_1 \rightarrow \infty$ and diffusion coefficients diverge $D(t) \rightarrow \infty$ (cf. Figs. 3 and 4); (ii) when temperature vanishes $\theta \rightarrow 0$ but time is fixed $t = t_i$, the diffusion saturates on the ballistic front $D(t_i) \rightarrow D_b(t_i)$ (see Fig. 6); and (iii) if temperature is finite $\theta = \text{const}$ but time tends to infinity $t \rightarrow \infty$, the diffusion must eventually be normal, i.e., $D(t) = D = \text{const}$ (cf. Fig. 3).

VII. CONCLUSION

In this work we revisited the problem of diffusion in a tilted periodic potential to consider the riddle of the weak-thermal-noise limit in this system. It has been investigated for over 20 years; however, it is still not entirely resolved and there

are many contradictory results in the literature. The reason behind it lies in the fact that in the low-temperature regime this system is weakly nonergodic, i.e., it exhibits an extremely slow relaxation towards its steady state. Therefore, asymptotic analytical methods should be employed, however, these have not yet been developed.

We exploited the state-of-the-art computer simulations of a timescale spanning nine orders of magnitude of the characteristic unit of time to study behavior of the diffusion coefficient $D(t)$ when the temperature of the system goes down to zero $\theta \rightarrow 0$. We found that for a given damping γ , if temperature vanishes, the diffusion coefficient $D(t)$ in the long-time limit is divergent $D(t) \rightarrow \infty$ when the constant force is in the range $f_1(\gamma) < f < f_3$, i.e., the velocity bistability effect occurs; otherwise it tends to zero $D(t) \rightarrow 0$. This result is consistent with the diffusive behavior observed for the deterministic counterpart of the studied system. In contrast, the statement that for the subcritical $[f_1, f_{gd,-}]$ and supercritical $[f_{gd,+}, f_3]$ biases the stationary diffusion coefficient tends to zero $D \rightarrow 0$ when temperature vanishes is not compatible with the deterministic dynamics in these regimes. In such a limit the lifetime of ballistic diffusion diverges to infinity and consequently the diffusion coefficient does not reach its stationary value.

We showed that the magnitude of the constant bias f modifies qualitatively the nonmonotonic dependence of the finite-time diffusion coefficient $D(t_i)$ on temperature θ . In the critical range $[f_{gd,-}, f_{gd,+}]$ predicted by a two-state theory it displays only one minimum, whereas for the subcritical $[f_1(\gamma), f_{gd,-}]$ and supercritical $[f_{gd,+}, f_3]$ areas both local minima and maxima are attainable. Finally, we demonstrated that for a given temperature of the system the magnitude of the stationary diffusion coefficient D as a function of the bias f is ruled by the relation between the number of locked and running trajectories. In particular, we identified that the diffusion D is maximal when the locked and running trajectories are equiprobable, i.e., when the difference $Q = 1 - |p_l - p_r|$ attains its maximum $Q = 1$ (cf. Fig. 5).

Summarizing, our numerical results allowed us to draw an inference about the conundrum of the weak-thermal-noise limit for diffusion in a tilted periodic potential. These findings for the paradigmatic model of nonequilibrium statistical physics can be applied, e.g., to Josephson junctions and cold atoms dwelling in optical lattices.

ACKNOWLEDGMENT

This work was supported by the NCN Grant No. 2017/26/D/ST2/00543 (J.S.).

-
- [1] S. H. Strogatz, *Nonlinear Dynamics and Chaos: With Applications to Physics, Biology, Chemistry and Engineering*, 2nd ed. (CRC, Boca Raton, 2015).
 - [2] E. Ott, *Chaos in Dynamical Systems*, 2nd ed. (Cambridge University Press, Cambridge, 2002).
 - [3] A. N. Pisarchik and U. Feudel, *Phys. Rep.* **540**, 167 (2014).
 - [4] G. L. Lamb, *Elements of Soliton Theory* (Wiley, New York, 1980).
 - [5] F. Sagués, J. M. Sancho, and J. García-Ojalvo, *Rev. Mod. Phys.* **79**, 829 (2007).
 - [6] R. Benzi, A. Sutera, and A. Vulpiani, *J. Phys. A: Math. Gen.* **14**, L453 (1981).
 - [7] L. Gammaitoni, P. Hänggi, P. Jung, and F. Marchesoni, *Rev. Mod. Phys.* **70**, 223 (1998).
 - [8] A. S. Pikovsky and J. Kurths, *Phys. Rev. Lett.* **78**, 775 (1997).

- [9] B. Lindner, J. García-Ojalvo, A. Neiman, and L. Schimansky-Geier, *Phys. Rep.* **392**, 321 (2004).
- [10] P. Hänggi and F. Marchesoni, *Rev. Mod. Phys.* **81**, 387 (2009).
- [11] J. Spiechowicz, P. Hänggi, and J. Łuczka, *Phys. Rev. E* **90**, 032104 (2014).
- [12] L. Machura, M. Kostur, P. Talkner, J. Łuczka, and P. Hänggi, *Phys. Rev. Lett.* **98**, 040601 (2007).
- [13] J. Nagel, D. Speer, T. Gaber, A. Sterck, R. Eichhorn, P. Reimann, K. Ilin, M. Siegel, D. Koelle, and R. Kleiner, *Phys. Rev. Lett.* **100**, 217001 (2008).
- [14] A. Slapik, J. Łuczka, P. Hänggi, and J. Spiechowicz, *Phys. Rev. Lett.* **122**, 070602 (2019).
- [15] J. Spiechowicz, P. Hänggi, and J. Łuczka, *New J. Phys.* **21**, 083029 (2019).
- [16] J. Spiechowicz and J. Łuczka, *Sci. Rep.* **7**, 16451 (2017).
- [17] J. Spiechowicz and J. Łuczka, *Chaos* **29**, 013105 (2019).
- [18] R. Metzler, J. H. Jeon, A. G. Cherstvy, and E. Barkai, *Phys. Chem. Chem. Phys.* **16**, 24128 (2014).
- [19] H. Risken, *The Fokker-Planck Equation: Methods of Solution and Applications* (Springer, Berlin, 1996).
- [20] A. Barone and G. Paternò, *Physics and Application of the Josephson Effect* (Wiley, New York, 1982).
- [21] W. T. Coffey, Y. P. Kalmykov, and J. T. Waldron, *The Langevin Equation*, 2nd ed. (World Scientific, Singapore, 2004), Secs. 5 and 7–10.
- [22] P. Fulde, L. Pietronero, W. R. Schneider, and S. Strässler, *Phys. Rev. Lett.* **35**, 1776 (1975); W. Dieterich, I. Peschel, and W. R. Schneider, *Z. Phys. B* **27**, 177 (1977); T. Geisel, *Solid State Commun.* **32**, 739 (1979).
- [23] G. Grüner, A. Zawadowski, and P. M. Chaikin, *Phys. Rev. Lett.* **46**, 511 (1981).
- [24] S. Denisov, S. Flach, and P. Hänggi, *Phys. Rep.* **538**, 77 (2014).
- [25] R. Kubo, *Rep. Prog. Phys.* **29**, 255 (1966).
- [26] P. Hänggi, J. Łuczka, and J. Spiechowicz, *Acta Phys. Pol. B* **51**, 1131 (2020).
- [27] H. Vollmer and H. Risken, *J. Phys. B* **52**, 259 (1983).
- [28] J. Spiechowicz and J. Łuczka, *Phys. Rev. E* **91**, 062104 (2015).
- [29] T. Guerin and D. S. Dean, *Phys. Rev. E* **95**, 012109 (2017).
- [30] J.-M. Zhang and J.-D. Bao, *Phys. Rev. E* **95**, 032107 (2017).
- [31] F. Kindermann, A. Dechant, M. Hohmann, T. Lausch, D. Mayer, F. Schmidt, E. Lutz, and A. Widera, *Nat. Phys.* **13**, 137 (2017).
- [32] D. Kim, C. Bowman, J. T. Del Bonis-O'Donnell, A. Matzavinos, and D. Stein, *Phys. Rev. Lett.* **118**, 048002 (2017).
- [33] L. P. Fisher, P. Pietzonka, and U. Seifert, *Phys. Rev. E* **97**, 022143 (2018).
- [34] C. Cheng, M. Cirillo, G. Salina, and N. Gronbech-Jensen, *Phys. Rev. E* **98**, 012140 (2018).
- [35] A. Dechant, F. Kindermann, A. Widera, and E. Lutz, *Phys. Rev. Lett.* **123**, 070602 (2019).
- [36] I. Goychuk, *Phys. Rev. Lett.* **123**, 180603 (2019).
- [37] I. Goychuk and T. Poschel, *Phys. Rev. E* **102**, 012139 (2020).
- [38] K. Białas, J. Łuczka, P. Hänggi, and J. Spiechowicz, *Phys. Rev. E* **102**, 042121 (2020).
- [39] N. J. López-Alamilla, M. W. Jack, and K. J. Challis, *Phys. Rev. E* **102**, 042405 (2020).
- [40] V. H. Purrello, J. L. Iguain, V. Lecomte, and A. B. Kolton, *Phys. Rev. E* **102**, 022131 (2020).
- [41] B. Lindner, M. Kostur, and L. Schimansky-Geier, *Fluct. Noise Lett.* **1**, R25 (2001).
- [42] P. Reimann, C. Van den Broeck, H. Linke, P. Hänggi, J. M. Rubi, and A. Pérez-Madrid, *Phys. Rev. Lett.* **87**, 010602 (2001).
- [43] P. Reimann, C. Van den Broeck, H. Linke, P. Hänggi, J. M. Rubi, and A. Pérez-Madrid, *Phys. Rev. E* **65**, 031104 (2002).
- [44] J. C. Latorre, G. A. Pavliotis, and P. R. Kramer, *J. Stat. Phys.* **150**, 776 (2013).
- [45] L. Cheng and N. K. Yip, *Physica D* **297**, 1 (2015).
- [46] K. Proesmans and B. Derrida, *J. Stat. Mech.* (2019) 023201.
- [47] G. Constantini and F. Marchesoni, *Europhys. Lett.* **48**, 491 (1999).
- [48] K. Lindenberg, A. M. Lacasta, J. M. Sancho, and A. H. Romero, *New J. Phys.* **7**, 29 (2005).
- [49] I. G. Marchenko and I. I. Marchenko, *Europhys. Lett.* **100**, 50005 (2012).
- [50] B. Lindner and I. M. Sokolov, *Phys. Rev. E* **93**, 042106 (2016).
- [51] I. G. Marchenko, I. I. Marchenko, and V. I. Tkachenko, *JETP Lett.* **106**, 242 (2017).
- [52] I. G. Marchenko, I. I. Marchenko, and V. I. Tkachenko, *JETP Lett.* **109**, 671 (2019).
- [53] J. Spiechowicz and J. Łuczka, *Phys. Rev. E* **101**, 032123 (2020).
- [54] J. Spiechowicz and J. Łuczka, *Phys. Rev. E* **104**, 024132 (2021).
- [55] J. Spiechowicz, M. Kostur, and Ł. Machura, *Comput. Phys. Commun.* **191**, 140 (2015).
- [56] E. Platen and N. Bruti-Liberati, *Numerical Solution of Stochastic Differential Equations with Jumps in Finance* (Springer, Berlin, 2011).
- [57] J. Spiechowicz, J. Łuczka, and P. Hänggi, *Sci. Rep.* **6**, 30948 (2016).
- [58] M. Reiner, *Phys. Today* **17** (1), 62 (1964).